

# Medicinal Plant Extract Mediated Green Synthesis of Metallic Nanoparticles: A Review

Sudip Some<sup>1\*</sup>, Samanwita Das<sup>2</sup>, Rittick Mondal<sup>3</sup>, Moumita Gangopadhyay<sup>2</sup>, Goutam K. Basak<sup>4</sup> DOI: 10.18811/ijpen.v7i02.2

## ABSTRACT

The use of medicinal plant resources in the biosynthesis of metallic nanoparticles (MNPs) is remarkable in nanobiotechnology for its unique physicochemical and biological properties such as morphological diversity, large surface area by volume proportion, conductivity, stability, dispersity, and toxicity to microbes, or cancerous cells. Active phytochemicals or bioactive compounds in various medicinal plants such as flavonoids, phenolic acids, terpenoids, steroids, ascorbic acids etc. are capable of the bio-fabrication of various MNPs during the green synthesis. The biosynthesis method has a great potential to improve the manufacture of nanoparticles (NPs) without using any harmful and costly materials or chemicals that have been widely used in other traditional processes. The present review aims to describe the biosynthesis of metallic NPs using medicinal plant extract as a reducing and stabilizing agent. This review also focuses on the current state of various characterization techniques and basic features of various NPs and explores their possible uses in various biomedical sectors shortly.

**Keywords:** Antimicrobials, Green synthesis, Metallic nanoparticles, Medicinal plants, Nanobiotechnology, Phytochemicals.

*International Journal of Plant and Environment* (2021);

ISSN: 2454-1117 (Print), 2455-202X (Online)

## INTRODUCTION

Nanoscience is the study of materials within the nanoscale dimension ( $10^{-9}$  meter) and deals with their size and structure-dependent characteristics related to the appearance of individual atoms or molecules or variations relevant to the bulk content. The exceptional features of nanomaterials have been affected by the variance in their precise characteristic features, including morphology, stability, conductivity, optical, and catalytic properties. The biomolecules functionalized NPs have been used to inactivate the surface defect, leading to a decrease in cell line toxicity. According to the chemical composition, nanomaterials have been classified into four types which include inorganic-based nanomaterials (IBNs), organic-based nanomaterials (OBNs), carbon-based nanomaterials (CBNs), and composite-based nanomaterials (COBNs) (Rawani *et al.*, 2013; Wang and Wang, 2014; Behravan *et al.*, 2019). It is a fundamental construction block of this technology and has excellent benefits by connecting between bulk and atoms or molecules (Thakkar *et al.*, 2010; Khan *et al.*, 2017a). NPs are commonly used in various biomedical fields as antimicrobials, anti-cancerous agents, biosensors, drug delivery and DNA analysis tools, and also in the wastewater treatment plant, moreover as a catalyst for various physicochemical and biological reactions (Park, 2003; Bora and Dutta, 2014; Zhang *et al.*, 2016). Inorganic-based NPs have been classified into two major categories, i.e., metallic NPs and metal oxide NPs (Jeevanandam *et al.*, 2018). Scientists and researchers have drawn their keen interest in this cutting edge technology to synthesize different metallic nanoparticles which include Silver nanoparticles (AgNPs), Gold nanoparticles (AuNPs), Copper nanoparticles (CuNPs), Palladium nanoparticles (PdNPs), and Platinum nanoparticles (PtNPs) having their versatile applications (Kanchana *et al.*, 2010; Umer *et al.*, 2014; Tippayawat *et al.*, 2016; Thirumurugan *et al.*, 2016; Ocsoy *et al.*, 2017b). Top-down and bottom-up approaches are two significant ways of synthesizing various NPs (Fig. 1). The top-down technique includes a process of breaking down the bulk construction

<sup>1</sup>Department of Life Sciences, Chanchal Siddheswari Institution, Chanchal-732123, Malda, West Bengal, India

<sup>2</sup>Department of Biotechnology, Adamas University, Kolkata-700126, West Bengal, India

<sup>3</sup>Chemical Biology Laboratory, Department of Sericulture, Raiganj University, Raiganj-733134, Uttar Dinajpur, West Bengal, India

<sup>4</sup>Department of Microbiology, Raiganj University, Raiganj-733134, Uttar Dinajpur, West Bengal, India

**\*Corresponding author:** Sudip Some, Department of Life Sciences, Chanchal Siddheswari Institution, Chanchal-732123, Malda, West Bengal, India, Mobile: +91-9474347483, Email: ssome.csi@gmail.com

**How to cite this article:** Some, S., Das, S., Mondal, R., Gangopadhyay, M., & Basak, G.K. (2021). Medicinal Plant Extract Mediated Green Synthesis of Metallic Nanoparticles: A Review. *International Journal of Plant and Environment*, 7(2), 119-132.

**Conflict of Interest:** None

**Submitted:** 17/02/2021 **Accepted:** 10/04/2021 **Published:** 15/07/2021

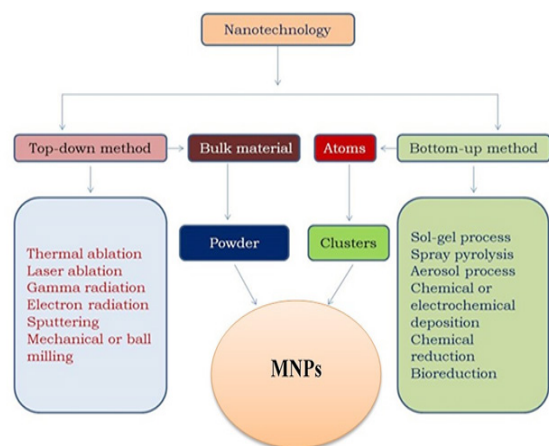


Fig. 1: Top-down and bottom-up approaches in nanotechnology

to generate tiny particles. Thermal or laser ablation, gamma radiation, electron radiation, sputtering, mechanical, or ball milling are common physical methods involved in the top-down method (Kulkarni and Muddapur, 2014). The bottom-up method provides an alternative route either combined with the top-down approach or its involvement in the synthesis of material through atom by atom, and/or molecule by molecule through the sol-gel method, spray pyrolysis, aerosol process, chemical or electrochemical deposition, and chemical reduction or biological-reduction (Pantidos and Horsfall, 2014).

The physical system applied in the top-down method is highly expensive and time-consuming. The involvement of some toxic materials such as dimethyl formamide, hydrazine, and sodium borohydride is a major disadvantage in the chemical reduction method (Iravani *et al.*, 2014).

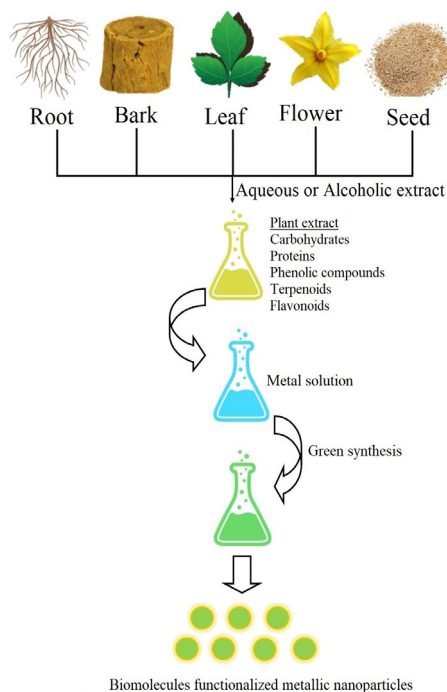
Conventionally, metallic nanoparticles (MNPs) have been synthesized by the reduction of metal ions in presence of toxic chemicals as well as synthetic stabilizers. But its application in biomedical sectors has been hampered by toxicity issues. The biosynthesis of NPs using different biological entities has been explored as an economical and environmental-friendly method and which is the substitute for the traditional physical and chemical methods. Medicinal plant extract mediated synthesis of NPs is an approach in green chemistry that links nanotechnology and plant biotechnology. Antimicrobial drug resistance in pathogenic microorganisms is one of the most serious universal public health problems in this century. The effectiveness of chemotherapy wanes for several causes, including the emergence of drug resistance in parasites or cancer cells. MNPs have a wide range of applications, but their antibacterial, anti-tumorigenic, and anti-inflammatory properties are the most explored and desired. In this context, various NPs were biosynthesized and reported simultaneously in the literature. Full elaboration goes beyond the reach of this inquiry as the present review is unique to selected MNPs. Thus, this present article focuses on medicinal plant extract mediated biosynthesis of MNPs, biophysical characterization of NPs and their versatile biocidal properties.

## BIOSYNTHESIS OF METALLIC NANOPARTICLES

Biosynthesis of MNPs has been emerged as the most promising area in nanotechnology by wide involvements of natural products. NPs have been synthesized using different medicinal plants, microorganisms, fungi, and algae in green synthesis methods. Natural products comprise a range of flavonoids, phenolic compounds, terpenoids, alkaloids, polysaccharides, proteins, enzymes, and amino acids that reduce and stabilizing agents. These phytochemicals in medicinal plants can also act as a capping agent, which performs a crucial role in the biosynthesis of NPs by providing a scaffold without using chemicals from outside (Baldemir *et al.*, 2017; Ocoy *et al.*, 2017a; Ovais *et al.*, 2018 Koca *et al.*, 2020). The biosynthesis process depends on several reaction parameters, including concentration and quantity of the metal salt, the quantity of plant extract, pH conditions, temperature, and reaction time (Table 1). The size distribution of biosynthesized MNPs has been recognized from the spectroscopic method. A comparative investigation has been carried out to explore the effects of

different AgNO<sub>3</sub> concentrations on the preparation of AgNPs. It is reported that the UV-vis spectra of AgNPs were achieved at various AgNO<sub>3</sub> concentrations, whereas the plant extract concentration was kept constant (7.5 mL) at 90°C for 2 hours. It was perceived that, as the concentration of AgNO<sub>3</sub> increased, the maximum absorbance ( $\lambda_{max}$ ) shifted from 447 nm (1 mM) to 455 nm (5 mM), indicating a slight increase in particle size (Khan *et al.*, 2013). The SPR band of CuNPs became prominent with increasing the extract concentration, as reported by Amaliyah *et al.* (2020) using both sonication and stirring methods, and the highest peak intensity was reached at the maximum extract concentration. They observed that, when reaction temperatures dropped, SPR absorption increased, indicating the production of larger particles in both stirring and sonication methods and acidic pH can cause inactivity of specific biomolecules present in the plant extract led to the smaller size of the produced NPs. Jamdade *et al.* (2019) reported that the intensity of the UV-spectra increased until 5 hours, after which there was no significant increase, indicating that the bioreduction process had been completed in 5 hours. The facile one-pot green synthesis of MNPs using medicinal plant extract is presented in Scheme-1.

The earlier study on the TEM micrograph of the biosynthesized AgNPs using *Lampranthus coccineus* aqueous plant extract or hexane extract showed an average particle size of 10.12 nm or 27.89 nm respectively. Whereas, the same volume of *Malephora lutea* aqueous plant extract or hexane extract was used and the particle size of 8.91 nm or 14.48 nm was achieved (Haggag *et al.*, 2019). The rate of plant extract-mediated green synthesis of different MNPs is also very high as compared to microbial-mediated synthesis. Some *et al.* (2020) reported that the biosynthesis of nano-silver using leaf extract of the mulberry plant was established by the changing of colour of the solution



**Scheme 1:** Medicinal plant extract mediated biosynthesis of metallic nanoparticles

from yellowish to light brown within 10 minutes. The light brown colour was changed to dark brown which confirmed the accomplishment of the reaction after 1 hour. In a separate study, Matei *et al.* (2020) described that the synthesis of AgNPs was confirmed after 24 hours incubation of cell-free culture of Lactic Acid Bacteria (LAB) with aqueous AgNO<sub>3</sub> solution by changing the color to dark brown. The use of plant extracts further reduces the expenses of microbial culture, thereby improving the viability for the synthesis of NPs using microorganisms. The biomolecules in the green extracts perform a significant role in regulating the morphological variations of MNPs. The biosynthesis process involves the use of fewer reagents and non-hazardous precursors. The entire reaction occurs in an aqueous medium at room temperature, unlike as compared with conventional methods (Das *et al.*, 2017; Aritonang *et al.*, 2019). The biosynthesis of numerous MNPs using medicinal

plant extracts has been explored by eminent scientists and researchers across the globe, which is presented in Table 2. The plant extract has been prepared from different parts of the medicinal plants. A study has shown that aqueous leaf extracts of *Dendropanax morbifera* Léveillé containing AgNO<sub>3</sub> solution became dark brown after 1 hour, but the solutions containing HAuCl<sub>4</sub> turned dark ruby red in 3 minutes at 80°C. The size and morphology of NPs have been varied based on the nature of plant extract and metal salt used (Wang *et al.*, 2016).

An earlier study has shown that isoquercetin, sophoraisoflavanone A, and cyclomorusin (flavonoids), mangiferin xanthonoid and gallic acid (phenolic compounds), and kazinol B and stigmasterol are recognized as predominant phytochemicals in the leaf of *Morus indica* L. V1 and performed a pivotal role for the bio-reduction of Ag<sup>+</sup> to form AgNPs. In the biosynthesis mechanism, AgNO<sub>3</sub> dissociates into Ag<sup>+</sup> (silver) and NO<sub>3</sub><sup>-</sup> (nitrate) ions.

**Table 1:** Summary of protocol for biosynthesis of metallic nanoparticles

MNPs	Metal salt used	Concentration(s) of metal salt and/ quantity	Biogenic sources	Quantity of plant extract	pH	Temperature	Reaction time	References
AgNPs	AgNO <sub>3</sub>	1 mM; 9 mL	<i>Prosopis farcta</i> (Banks & Sol.) <i>J. F. Macbr.</i>	100–140 µL	-	50–70°C	4 hours	Salari <i>et al.</i> , 2019
AgNPs	AgNO <sub>3</sub>	1 mM; 90 mL	<i>Nigella arvensis</i> L.	10 mL	-	Environment temperature	5–120 minutes	Chahardoli <i>et al.</i> , 2018
AgNPs	AgNO <sub>3</sub>	1-5.5 mM; 90-99 mL	<i>Pulicaria glutinosa</i> (Boiss.) Jaub. & Spach	1–10 mL	-	90°C	2 hours	Khan <i>et al.</i> , 2013
AuNPs	HAuCl <sub>4</sub> ·3H <sub>2</sub> O	1 mM; 1 mL	<i>Euphorbia peplus</i> L.	99 mL	-	Room temperature	-	Ghranh <i>et al.</i> , 2019
AuNPs	HAuCl <sub>4</sub> ·3H <sub>2</sub> O	1 mM; 20 mL	<i>Origanum vulgare</i> L.	0.25–2 mL	2.5–3.2	85°C	1 minute	Benedec <i>et al.</i> , 2018
AuNPs	HAuCl <sub>4</sub> ·3H <sub>2</sub> O	1 mM; 10 mL	<i>Euphrasia officinalis</i> f. <i>curta</i> Fr.	5 mg/10 mL	-	37°C	3 hours	Liu <i>et al.</i> , 2019
CuNPs	CuSO <sub>4</sub> ·5H <sub>2</sub> O	100 mM; 25 mL	<i>Piper retrofractum</i> Vahl	20–100 mL	4–10	25–80°C	-	Amaliyah <i>et al.</i> , 2020
CuNPs	CuSO <sub>4</sub> ·5H <sub>2</sub> O	1 mM; 95 mL	<i>Gnidia glauca</i> (Fresen.) Gilg and <i>Plumbago zeylanica</i> L.	5 mL each	-	100°C	15–60 minutes	Jamdade <i>et al.</i> , 2019
PdNPs	PdCl <sub>2</sub>	1 mM; 50 mL	<i>Camellia sinensis</i> (L.) Kuntze	50 mL	7.5-5.6	40°C	2 hours	Azizi <i>et al.</i> , 2017
PdNPs	PdCl <sub>2</sub>	1mM; 100 mL	<i>Evolvulus alsinoides</i> (L.) L.	10 mL	-	60°C	6 hours	Gurunathan <i>et al.</i> , 2015
PtNPs	H <sub>2</sub> PtCl <sub>6</sub> ·6H <sub>2</sub> O	1mM; 95 mL	<i>Dioscorea bulbifera</i> L.	5 mL	-	100°C	6 hours	Ghosh <i>et al.</i> , 2015

**Table 2:** Medicinal plants used in green synthesis of MNPs

Plants Name	Used part	NPs synthesized	Shape	Size (nm)	References
<i>Allium sativum</i> L.	B	Ag	Spherical	3–6	Otunola <i>et al.</i> , 2017
<i>Bacopa monnieri</i> (L.) Wettst.	L	Pt	Spherical	5–20	Nellore <i>et al.</i> , 2013
<i>Borago officinalis</i> L.	L	Ag	Spherical and Hexagonal	30–80	Singh <i>et al.</i> , 2016
<i>Brassica oleracea</i> L.	I	Cu	Spherical	~ 4.8	Prasad <i>et al.</i> , 2016
<i>Camellia sinensis</i> (L.) Kuntze	L	Ag	Spherical	27.9–50.2	Kharabi Masooleh <i>et al.</i> , 2019
<i>Cannabis sativa</i> L.	St	Au and Ag	Spherical	Au: 12–18 Ag: 20–40	Singh <i>et al.</i> , 2018
<i>Capsicum frutescens</i> L.	F	Ag	Spherical	3–18	Otunola <i>et al.</i> , 2017
<i>Dendropanax morbifera</i> Léveillé	L	Au and Ag	Polygonal and Hexagonal	Au: 100–150 Ag: 10–20	Wang <i>et al.</i> , 2016
<i>Eleutherococcus senticosus</i> (Rupr. & Maxim.) Maxim.	St	Ag and Au	Cubical	Ag: 126 Au: 189	Abbai <i>et al.</i> , 2016
<i>Euphrasia officinalis</i> f. <i>curta</i> Fr.	L	Au and Ag	Quasi-spherical	Au: 49.72 ± 1.2 Ag: 40.37 ± 1.8	Singh <i>et al.</i> , 2017
<i>Glycyrrhiza uralensis</i> Fisch.	R	Au and Ag	Spherical	Au: 12.25 Ag: 8.01	Huo <i>et al.</i> , 2018
<i>Justicia glauca</i> Rottler	L	Au	Hexagonal and Spherical	~32.5 ± 0.25	Emmanuel <i>et al.</i> , 2017
<i>Phyllanthus emblica</i> L.	Sd	Pd	Spherical	28 ± 2	Dinesh <i>et al.</i> , 2017
<i>Punica granatum</i> L.	Sd	Cu	Semi-Spherical	40–80	Nazar <i>et al.</i> , 2018
<i>Selaginella myosurus</i> Alston	Wp	Ag	Spherical	58.81	Kedi <i>et al.</i> , 2018
<i>Swertia paniculata</i> Wall.	Wp	Ag	Spherical	31–44	Ahluwalia <i>et al.</i> , 2018
<i>Zingiber officinale</i> Rosc.	Rz	Ag	Spherical	3–22	Otunola <i>et al.</i> , 2017

Abbreviations: B: Bulb; F: Fruit; I: Inflorescence; L: Leaf; R: Root; Rz: Rhizome; Sd: Seed; St: Stem; Wp: Whole plant

Two H<sup>+</sup> ions release from flavonoid compounds and two O<sup>-</sup> reduce two Ag<sup>+</sup> to form Ag<sup>0</sup>. Another study suggested that -OH and -COOH groups in gallic acid were accountable for the reduction of Ag<sup>+</sup> to Ag<sup>0</sup>. Gallic acid was oxidized into its corresponding compound quinone and absorbed through electrostatic interaction between carboxylic acid groups of phenolic acid on the surface of the NPs. Moreover, phenolic acid molecules on the surface of NPs form H bonds with neighboring molecules (Some *et al.*, 2019; 2020). Banerjee and Nath (2015) reported that -OH, -C=O, and -NH functional groups in the unique phytochemicals which include dibenzoyl-L-tartaric acid, 2,4-di-tert-butylphenol and 2,4-dichloro-6-phenyl-1,3,5-triazine and performed as reducing and stabilizing agents in the biosynthesis of AgNPs and which were isolated from the bark extract of *Saraca asoca* (Roxb.) Willd. Ahmad *et al.* (2019) proposed that Gallic acid interacts with Au<sup>+3</sup> ions owing to binding affinity and discharges electrons which reduce the Au<sup>3+</sup> into Au<sup>0</sup>. In this reaction, a gold intermediate complex was formed, and which was further oxidized to form quinones and AuNPs. Quinones might be attached to the AuNPs surface by carbonyl groups and created a repulsive force that prevents their agglomeration and improved their long-term colloidal stability. Formation of the AuNPs was finished by complete

reduction of Au<sup>+3</sup> and which was specified the colour change of the solution from yellow to red (Ismail *et al.*, 2018). Hazarika *et al.* (2017) observed that the formation of PdNPs is confirmed by the change of colour of the solution from orange to dark brown after adding the plant extract to Palladium (II) acetate [Pd(OAc)<sub>2</sub>] solution. In the presence of plant extract the formation of Platinum (II) was identified by the change in the color, which turned into brown from light yellow and for PtNPs, it turned to black from brown (Thirumurugan *et al.*, 2016). The formation of CuNPs is ensured by changes of color of the solution from blue to pale bluish-green (Rajesh *et al.*, 2018). The plausible mechanism for the biosynthesis of MNPs is presented in Fig. 2.

## CHARACTERIZATION OF METALLIC NANOPARTICLES

Different instrumental methods have been applied to understand the shape, size, crystallinity, elemental conformation, and other biophysical features of NPs. Ultraviolet-visible spectrophotometer, Fourier transform infrared spectroscopy (FT-IR), X-ray photoelectron spectroscopy (XPS), energy-dispersive X-ray spectroscopy (EDS/EDX), Raman spectroscopy, different electron microscopy (TEM/HRTEM/SEM), atomic force

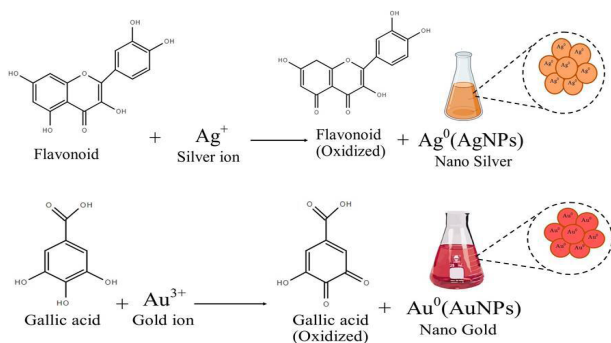


**Fig. 2:** Phytochemical mediated reduction of metal ions and MNPs synthesis

microscopy (AFM), particle size analyzer, and X-ray diffraction (XRD) have been used as sophisticated instruments to characterize synthesized NPs (Joshi *et al.*, 2008; Mourdikoudis *et al.*, 2018; Mondal *et al.*, 2021).

### Spectroscopic Methods

UV-vis spectroscopy is a suitable and dependable method for the presumptive characterization of synthesized NPs. This spectroscopic method quantitatively measures the concentrations of the absorber in the solutions containing the ions of transition metal. It has also been used to monitor the synthesis and stability of NPs by determining the absorbance at the UV-visible spectral region (Sastry *et al.*, 1998; Sooväli *et al.*, 2006). Each NP has a unique optical property, which makes them strongly interact with specific wavelengths of light. The interaction of synthesized MNPs and light contributes to a polarization of free conduction of electrons ( $e^-$ ) in respect to the much stronger ionic center of NPs, resulting in electron dipolar oscillation and the presence of a surface plasmon resonance (SPR) band at a wavelength of light (Some *et al.*, 2019). In addition, UV-vis spectroscopy is a rapid, easy, simple, sensitive, and selective analytical technique for the measurement of different types of NPs within a short period (Begum *et al.*, 2018). In a study, it was observed that maximum absorbance was recorded at 423 nm within 10 minutes in coconut water-mediated biosynthesis of nanosilver (Elumalai *et al.*, 2014). The spectrum of biosynthesized AuNPs using *Mentha piperita* oil showed a narrow peak, which was observed at 530 nm (Thanighaiarassu *et al.*, 2014). The *Alchornea laxiflora* leaves extract mediated green synthesized CuNPs displayed maximum absorption at 364 nm (Olajire *et al.*, 2018). Jeyapaul *et al.* (2018) confirmed that the SPR band displays a redshift value at 260 nm, which was established by the reduction of  $\text{Pt}^{4+}$  ions to form PtNPs. Azizi *et al.* (2017) conveyed that, *Camellia sinensis* extract mediated biogenic PdNPs showed a maximum absorbance peak at 410 nm. In this experiment, an aqueous extract of white tea displayed an intense absorption peak at 250 nm indicated the presence of flavonoids. But there is some limitation in this technique. The separate peaks for NPs having different sizes are not observed in UV-vis spectroscopy. The polydisperse colloidal particles exhibited a wide SPR band in comparison with monodisperse colloidal particles that indicate a narrow band. At a high concentration of 10 mM, solute molecules in the solution can induce the specific distribution of

charges on their neighboring species. Therefore, AFM or TEM/SEM has been applied much more reliable techniques for further characterization of NPs (Tomaszewska *et al.*, 2013).

The FT-IR is another analytical method, which has been used to recognize the functional groups of biomolecules existing in plant extract and which is responsible for the bioreduction of metal salt. This analytical technique calculates the absorption of the infrared spectrum by the sample materials. The infrared absorption bands detect the molecular components of the sample. The absorption of the IR region of the spectrum by various molecules endorses shifts between the rotational and vibrational energy levels of the ground electronic energy state (Devaraj *et al.*, 2013; Song *et al.*, 2020). IR spectroscopy also provides the benefits of persistent activity and low downtime relative to gas chromatography and low expense and structural accuracy as opposed to mass spectroscopy. A sample IR beam is guided through the sample chamber in a traditional IR spectrophotometer and calibrated against a reference beam at each wavelength of the spectrum. The complete spectral zone must be scanned slowly to obtain a good quality spectrum (Doyle, 1992; Ismail *et al.*, 1997). IR peak at  $3333\text{ cm}^{-1}$  has identified the hydroxyl group (H-bonded OH stretch). The peak has been observed at  $2917\text{ cm}^{-1}$  conforms to asymmetric and symmetric stretching of methylene group ( $=\text{CH}_2$ ). The absorption bands at about 3400, 1650, 1595, 1400, and  $1100\text{ cm}^{-1}$  corresponded to C-H, C=O, -OH, C=C and C-OH groups (Murthy *et al.*, 2018). The peaks have been observed at  $1643\text{ cm}^{-1}$  and  $1629\text{ cm}^{-1}$  indicating the stretching vibration of alkenes ( $-\text{C}=\text{C}-$ ) and alpha, beta-unsaturated aldehydes, and ketones (C=O). The band above  $3417\text{ cm}^{-1}$  specified the occurrence of O-H and N-H stretching vibrations (Ranjitha *et al.*, 2018). Geetha *et al.* (2013) observed that, the flower extract of *Couroupita guianensis* Aubl. showed the absorption bands at 1648, 1383, 1288, and  $1073\text{ cm}^{-1}$  confirmed to  $-\text{C}=\text{C}-$  (stretch of alkynes), C-N (stretching vibration of aliphatic amines), C-O (stretch of alcohols) and C-N (stretching vibrations of aliphatic amines or alcohols/phenols). These functional groups were capable to reduce, and a new band seemed at  $1744\text{ cm}^{-1}$  which indicates the -OH group is changed into -CHO to reduce  $\text{Au}^{+++}$  to  $\text{Au}^0$ . Beg *et al.* (2018) ensured in their study that absorption bands at about 1545, 3250, 3158, 1732, and  $3565\text{ cm}^{-1}$  corresponded to COOH, NH, N-O, CO, and OH functional groups which performed as reducing and stabilizing agents in *Spathodea campanulata* P. Beauv. leaf extract mediated biosynthesis of AgNPs. Hassanien *et al.* (2018) described that; biosynthesized CuNPs displayed an extensive peak in  $3410\text{ cm}^{-1}$  owing to O-H groups. The absorption bands at 1028, 1783, 1615 and  $2949\text{ cm}^{-1}$  are associated with C-OH bending, C-H asymmetric stretching, C=O of aromatic rings, and C=C stretching respectively. The *Gloriosa superba* tuber extract displayed an absorption band at  $\sim 3300\text{ cm}^{-1}$ , which is precise for the hydroxyl group of alcoholic and phenolic compounds, which remain unchanged even after NPs synthesis. But the bands observed at 1049, 1218, 1369, and  $1737\text{ cm}^{-1}$  are specific for the C-O-C bond in ether, unassigned amide mode,  $\text{CH}_3$  bend, and the stretching of C=O bond remain altered after biosynthesis of PtNPs and PdNPs (Rokade *et al.*, 2018). FTIR frequency range and functional groups present in the plant extract are presented in Table 3.

**Table 3:** FTIR frequency range and functional groups present in the plant extract

Frequency range (cm <sup>-1</sup> )	Functional groups
3565	-OH (hydroxyl)
3410	-OH (hydroxyl)
3250	=NH <sub>2</sub> (amine)
3158	N-O
2949	C-H (asymmetric stretching)
1783	C=C (stretching)
1732	C=O (carbonyl)
1648	-C=C- (stretch of alkenes)
1615	C=O
1545	-COOH (carboxyl)
1383	C-N (stretching vibration of aliphatic amines)
1288	C-O (stretch of alcohols)
1073	C-N (stretching vibrations of aliphatic amines or alcohols/phenols).
1028	C-OH (bending)

The XPS is a quantitative spectroscopic technique focused on the photoelectric influence that can categorize the elements that occur within a substance or cover its surface, as well as its chemical condition and the total electronic configuration and intensity of the electronic state in the sample (Seah and Dench, 1979). Ajitha *et al.* (2015) reported the strong signal of Ag 3d (~370 eV) specifies the incidence of Ag metal. The C 1s band detected at a binding energy of ~285 eV attends as a reference to the correct binding energy shift and it also stems from biomolecules of leaf extract encapsulated to nano-silver. The spectrum also contains O (~531 eV), Cl (~198 eV), S (~163 eV) and P (~133 eV) elements in their corresponding binding energy sites due to the interface of bio-active compounds of leaf extract with AgNPs. Biosynthesized AuNPs have undoubtedly displayed the presence of oxygen (O 1s), carbon (C 1s) and gold (Au 4f) by their peaks centered around of 532, 284, and 85 eV, respectively. XPS data revealed that more hydroxyl groups (-C-OH) are expended to reduce a larger number of Au<sup>3+</sup> ions and decrease of C-O signal in AuNPs (where the concentration of HAuCl<sub>4</sub> was fixed at 5.3 mM) approves that hydroxyl groups contribute to the biosynthesis reaction (Rodriguez-Leon *et al.*, 2019). The high-resolution narrow scans (Pd 3d) of the biosynthesized PdNPs exhibited binding energy peaks at 335.26 and 340.6 eV corresponding to the spin-orbit splitting components Pd 3d 5/2 and Pd 3d 3/2, respectively, which is the characteristic of Pd in the zero-oxidation state. The PtNPs gave the Pt 4f 7/2 signal at 71.5 eV can be assigned to zero-valent platinum (Rajasekharreddy and Rani, 2014). The EDX has been used to identify the elemental composition of materials using an X-ray technique (Zheng *et al.*, 2011). Metallic nanosilver typically exhibits a normal optical absorption band at around 3KeV due to SPR. EDX data displayed strong silver and weak signals of chloride and carbon bands, which specify that the reduction of Ag<sup>+</sup> to Ag<sup>0</sup> may be originated from the bio-molecules involved in the surface of the

AgNPs (Velavan and Amargeetha, 2018). Hazarika *et al.* (2017) reported that, the incidence of Pd along with the signals of other elements such as N, O, and S in the spectra of EDX. Raman spectroscopy (RS) has been included under the family of spectral analyses made on molecular media based on inelastic scattering of monochromatic light (Javier, 2014). Green synthesized AgNPs have been characterized by Raman study in the range of 125 - 4000 cm<sup>-1</sup>. RS exhibited the prominent peaks at 673.53 cm<sup>-1</sup> (C-S, bending), 1035.87 cm<sup>-1</sup> (C = S, bending), 1359.92 and 1549 cm<sup>-1</sup> (N = N, stretching), and 2213.73 cm<sup>-1</sup> (C = C, stretching) (Sharma *et al.*, 2018). The IR spectra are the effect of absorption of definite frequencies of wavelength thus changes an electric dipole situation and displays IR bands. The RS confirms the electrical polarizability of molecules (Sharma *et al.*, 2009).

### Microscopic Methods

Transmission electron microscopy (TEM) is a microscopic method in which a beam of electrons is transmitted through a sample or specimen (preferably size less than 100 nm) to form an image. The image is magnified and displayed onto an imaging device which includes a photographic plate, fluorescent screen or a sensor such as a scintillator attached to a charge-coupled device (Asadabad and Eskandari, 2014). It has been broadly used as a technique to characterize the shape and size of NPs. The particles are placed by a drop onto the copper grid for analysis (Maji *et al.*, 2017a). Moodley *et al.* (2018) reported that the biosynthesized AgNPs are seemed well dispersed and spherical in shape using TEM. The investigation exposed the AgNPs to possess a narrow size distribution range with average sizes of 11 ± 4.3 nm and 9 ± 4.2 nm using freeze-dried and fresh leaf samples of *Moringa oleifera*. A high-resolution transmission electron microscopic (HRTEM) study observed that the biogenic PdNPs appeared flower-like aggregations and which were made up of the self-assembled discrete NPs appearing from multiple directions (Majumdar *et al.*, 2017). A study perceived that TEM pictures established the hexagonal and pentagonal shape of the synthesized PtNPs having in the size range of 10-30 nm (Dobrucka, 2019). In an investigation, volume mean diameter (VMD) and sauter mean diameter (SMD) of NPs were measured as 56.06 and 56.09 nm, which specifies the closer values of the two parameters with each other. The values are also specified that the biosynthesized NPs are spherical and confirmed by TEM (Kharabi Masooleh *et al.* 2019).

Field emission scanning electron microscopy (FE-SEM) is another tool for the morphological analysis of NPs. The sample is exposed in SEM to the high-energy electron beam and gives information about topography, morphology, composition, chemistry, the orientation of grains, crystallographic information (Akhta *et al.*, 2018). Before analysis NPs are sonicated thoroughly. Now it is placed on the coverslip and allowed to dry under vacuum at room temperature (Maji *et al.*, 2017b). In the microscopic study, SEM images offer an overall idea about the crystallographic properties of the biosynthesized AgNPs. The SEM data exposed the size of biogenic AuNPs was measured between 50-80 nm (Nasiri and Nasiri, 2016; Islam *et al.*, 2019). In the characterization of NPs, TEM is a better imaging tool, but SEM or T-SEM imaging in combination with EDX is a quick and practical instrumental technique to evaluate the morphology including size and elemental composition (Rades *et al.*, 2014).

SEM images revealed the cubical, spherical, and truncated triangular forms of the biosynthesized AgNPs. SEM images of the CuNPs also show the cubical and spherical structures, with an extended conformation. Biogenic AgNPs and CuNPs were 40–100 nm and 10–70 nm in size, respectively (Arya *et al.*, 2018). The AFM is a category of high-resolution scanning probe microscopes (SPM) in material science. The SPMs are premeditated to analyze the local properties, including height, friction, and magnetism (Sun, 2018). AFM study observed the two-dimensional image of biosynthesized AgNPs, and are monodispersed and spherical in shape with an average size range between 10–25 nm. The study also demonstrates three-dimensional and topographical images of AgNPs (Daphedar and Taranath, 2018). There are some limitations in AFM which include (i) It can only scan a single nano-sized image at a time of about 150 x 150 nm, (ii) They have a low scanning time which might cause thermal drift on the sample, (iii) The tip and the sample can be damaged during detection, and (iv) It has a limited magnification and vertical range (Mokobi, 2020).

### Diffraction and Light Scattering Study

XRD is a distinctive analytical technique for the determination of the crystallinity of NPs. The presence of intense peaks has confirmed the face-centered crystalline (fcc) nature of synthesized NPs (Bunaciu *et al.*, 2015). Some *et al.* (2020) conveyed the crystallinity of biogenic AgNPs which was directed in the range of  $20^\circ \leq 2\theta \leq 80^\circ$  at 40 keV using an X-ray diffractometer and operated at 9 kW and CuK $\alpha$  radiation ( $\lambda = 1.54056 \text{ \AA}$ ). The PowderX software has been used to calculate the lattice fringe of the crystals. Priyadarshini *et al.* (2018) showed the Bragg diffraction angle ( $2\theta$ ) at  $38^\circ$ ,  $44.5^\circ$ ,  $64.7^\circ$ , and  $77.7^\circ$  indexed to the 111, 200, 220, and 311 reflections of fcc nature of AgNPs. The crystalline nature of NPs is also detected from the selected area electron diffraction (SAED) pattern. A report was noted that four bright circular rings were consigned to (111), (200), (220) and (311) perceived in the SAED pattern were the characteristic reflections of fcc crystalline AgNPs and AuNPs (Abbai *et al.*, 2016; Singh *et al.*, 2017). The average size of NPs is measured by using Debye-Scherrer's equation (equation 3) (Singh and Vishwakarma, 2015).

$$D = K \lambda / (\beta \cos \theta) \quad (1)$$

Where D: size of crystallites (nm), K: 0.9 (shape factor),  $\lambda$ : wavelength of X-ray,  $\beta$ : full width at half maximum in radians of diffraction peak and  $\theta$ : Bragg diffraction angle (degree).

There are some limitations to the XRD study. X-ray does not interrelate very powerfully with lighter elements and the intensity is  $10^8$  times less than that of electron diffraction (Norton, 1937).

The particle size distribution of NPs has been measured by the dynamic light scattering (DLS) analyzer. It is based on the Brownian motion of dispersed particles. The relation between the speed of the particles and the particle size is agreed by the Stokes-Einstein equation (4). The speed of the particles is specified by the translational diffusion coefficient D (Achuthan *et al.*, 2011).

$$D = \frac{k_B T}{6\pi\eta r} \quad (2)$$

Where D: Translational diffusion coefficient [ $\text{m}^2/\text{s}$ ] - "speed of the particles",  $k_B$ : Boltzmann constant [ $\text{m}^2\text{kg}/\text{Ks}^2$ ], T: Temperature [K],  $\eta$ : Viscosity [Pa.s], r: Hydrodynamic radius [m]. Z-average size is a parameter used in DLS and is also known as the cumulative mean. It is the most stable and prime parameter produced by the method. It gives statistical data about the hydrodynamic size, kinetics of the aggregation process, polydispersity index (PDI), and surface properties of the NPs (Lim *et al.*, 2013). The hydrodynamic diameter ( $d_h$ ) is a sphere with the same coefficient of translational diffusion as the particle being measured, assuming a layer of hydration surrounding the particle or molecule. The hydrodynamic size of AgNPs is larger perhaps due to the encapsulation of bio-molecules (Anandalakshmi *et al.*, 2016). Zeta potential (ZP) measurement is an analytical technique for determining the stability of NPs by their surface charge in a colloidal system. NPs with ZP values  $> +30 \text{ mV}$  or  $< -30 \text{ mV}$  usually have high degrees of stability (Clogston and Patri, 2011). In a study by Chaudhuri *et al.* (2016), the particle size distribution was investigated through DLS and it was observed that the peaks were at 5.85 nm and 77.48 nm. PDI of biosynthesized AgNPs is 0.378 ( $< 1$ ) indicating that NPs are stable even after nine months of storage and uniform size range. The stability of biogenic AgNPs was examined by measuring ZP, and the value was recorded at  $-16.0 \text{ mV}$ . Some *et al.* (2020) conveyed that the nano-silver in Mueller Hinton broth (MHB) and DMEM/F12 medium had a hydrodynamic size of 25.3 and 50.5 nm, respectively. The  $d_h$  differs from the composition of the medium. There is some limitation in DLS study which includes temperature and solvent viscosity. The temperature must be retained constant, and solvent viscosity must be known for a reliable study. It is a low-resolution method that often cannot separate closely related molecules (Stetefeld *et al.*, 2016).

### BIOCIDAL PROPERTIES OF METALLIC NANOPARTICLES

Metallic NPs have been using in a wide range of products, and a number of them have been utilized as biocides due to their antimicrobial or antifungal properties (Mackevica *et al.*, 2016; Sangaonkar and Pawar, 2018). Smaller NPs are more effective

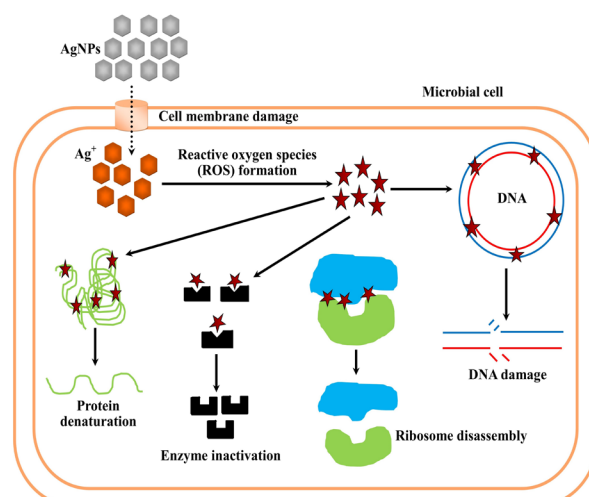


Fig. 3: Mode of action of AgNPs against microbial cell

than larger ones due to their easy dispersion into cells. After infiltration into the cell, NP generates reactive oxygen species (ROS) and free radicals that destroy the plasma membrane and nucleic acids and also trigger the inhibition of cell multiplication and program cell death (Siddiqi *et al.*, 2018) (Fig. 3). Wang *et al.* (2017) measured the toxicity effect of NPs on *Photobacterium phosphoreum* by superoxide production, measured by continuous flow chemiluminescence (CFCL) detection system. Apart from ROS production, NPs inhibit the enzyme activity of urease and DNA polymerase of bacteria (Khan *et al.*, 2017b).

Quorum sensing (QS) is a regulatory mechanism based on cell population density, utilizing tiny signaling molecules or autoinducers to achieve virulence gene expression and biofilm formation (Ghosh *et al.*, 2014). Ravindran *et al.* (2018) observed the counter QS and anti-biofilm properties of biosynthesized AgNPs against a nosocomial pathogen, *Serratia marcescens*. Shah *et al.* (2019) investigated the anti-QS and anti-biofilm properties of AgNPs against *Pseudomonas aeruginosa* PAO1.

### Antibacterial Activity

NPs have been studied broadly for their promising antimicrobial activity. A study observed the potential of biomolecules capped AgNPs against Gram-positive and Gram-negative bacteria such as *Bacillus cereus*, *Staphylococcus aureus* and *Escherichia coli*, *P. aeruginosa* (Maliszewska and Sadowski, 2009). Buszewski *et al.* (2018) revealed in their investigation that 8–48 nm bio-active nanosilver showed strong antimicrobial activity against *P. aeruginosa*, *S. aureus*, and *Proteus mirabilis*, followed by *E. coli*, *Klebsiella pneumoniae*, and *Bacillus subtilis*. Abbai *et al.* (2016) compared the antibacterial activity of *Eleutherococcus senticosus* (Rupr. & Maxim.) Maxim. (A noble medicinal plant, popularly known as Siberian ginseng) extract mediated biogenic AgNPs and AuNPs by the disc diffusion assay in terms of the zones of inhibition. In this investigation, AgNPs showed antibacterial potential against *S. aureus* (ATCC 6538), *Bacillus anthracis* (NCTC 10340), *Vibrio parahaemolyticus* (ATCC 33844), and *E. coli* (BL21) whereas AuNPs did not show any inhibitory activity against the above isolates. Another investigation observed the potential of *Mussaenda glabrata* (Hook.f.) Hutch. ex Gamble leaf extract mediated biogenic AgNPs and AuNPs by well diffusion pathway. These MNPs exhibited antimicrobial activity against both Gram-positive and Gram-negative bacteria such as *Bacillus pumilus* (MTCC 1640), *S. aureus* (MTCC 96), *P. aeruginosa* (MTCC 424) and *E. coli* (MTCC 443) (Francis *et al.*, 2017). Shende *et al.* (2015) concluded in their study that *Escherichia coli* was most sensitive to biogenic CuNPs followed by *K. pneumoniae*, *P. aeruginosa*, *Propionibacterium acnes* and *Salmonella typhi*. According to Kandi and Kandi (2015), NPs have been extensively used as an antibiotic alternative. Nanoscale materials' potential antimicrobial activity should be considered a fruitful signal of the utility as antimicrobial agents against multiple drug-resistant pathogens. Antony *et al.* (2011) suggested that bio-encapsulated AgNPs are more effective against pathogenic bacteria compared to chemically synthesized naked AgNPs. In a separate study, Chahar *et al.* (2018) exhibited that, bio-conjugated AgNPs, manufactured using different plant sources have cumulative antibacterial properties against *Salmonella enteric typhi* and *P. aeruginosa* than AgNPs synthesized by different chemicals. Nikitina *et al.* (2007) explored that, aqueous plant extracted

polyphenols exhibited significant bactericidal efficiency against Gram-negative and Gram-positive bacteria. Gallic acid is a predominant phenolic compound in the plant extract and exhibited antimicrobial efficacy by rupturing cell membranes due to the change of surface hydrophobicity and decrease of negative surface charges (Borges *et al.*, 2013). Therefore, medicinal plant extract mediated bio-encapsulated AgNPs warrant outstanding bacterial inhibition compares to naked AgNPs or bio-active compounds alone.

### Antifungal Activity

Apart from antibacterial properties, it has been reported by several investigations that NPs have strong antifungal activity. A study observed that AgNP showed strong antifungal activity against three different species of *Candida* like *C. albicans*, *C. glabrata* and *C. tropicalis* (Khan and Mushtaq, 2016). Bhagat *et al.* (2018) studied the antifungal experiment using the food poisoning technique. They observed that the growth of mycelia of fungi like *Bipolaris specifera*, *Fusarium oxysporum*, *Aspergillus niger*, and *Curvularia lunata* was inhibited by nanosilver treatment. Wani *et al.* (2013) investigated that; AuNPs showed fungicidal activity against *Candida* sp. through inhibiting H (+) -ATPase mediated pumping mechanisms. It was demonstrated that the AgNPs strongly inhibited the fungal growth of *Alternaria alternata* and *Botrytis cinerea* by damaging cell walls compared with CuNPs and Ag/CuNPs (Ouda, 2014). In another experiment CuNPs at the concentration 450 mg/L inhibit the 93.98% growth of *Fusarium* sp. in 9 days incubation period (Viet *et al.*, 2016). Therefore, NPs may be used as a wonderful broad-spectrum antifungal drug to control human and plant pathogenic fungi.

### Cytotoxicity

Biosynthesized NPs have an extensive range of applications in nanobiotechnology. Due to its fundamental properties, stability, and biocompatibility, it has been employed as a drug delivery vehicle in the biomedical field. Hybrid MNPs (Au-Ag) have a robust toxic effect against different carcinoma cell lines like HCT116, 4T1, HUH7, and HEK293 (Katifelis *et al.*, 2018). Selvi *et al.* (2016) found the cytotoxic potentiality of AgNPs against MCF-7 breast cancer cell line by an MTT assay. The MTT assay is a colorimetric analytical technique to assess cell viability. The assay analyzes the reduction of a yellow dye MTT (3-(4,5-dimethylthiazol-2-yl)-2,5-diphenyltetrazolium bromide) to produce an insoluble blue product formazan by a mitochondrial enzyme, succinate dehydrogenase (Riss *et al.*, 2013). Inflammatory reactions and cell death are both regulated by caspases enzymes. In an investigation, the amount of caspase 3 and 9 production in AgNP and extract-treated MCF-7 cells was compared to the untreated control group to confirm the apoptosis or program cell death. AgNPs caused DNA damage, endoplasmic reticulum stress, protein misfolding, and apoptosis by activating caspases 3 and 9 and other ROS. Caspase 3 has shown to cleave and translocate caspase-activated DNase (CAD) upon activation, resulting in DNA fragmentation (Ullah *et al.*, 2020). The intracellular apoptosis is stirred by the release of the mitochondrial cytochrome C and the loss of mitochondrial membrane potential ( $\Delta\Psi_m$ ). A study has shown that conjugation with papain-inspired gold nanoparticles (5F-PpGNPs) significantly augmented the potency of 5-Fluorouracil (5-FU) by acting synergistically. As a result,



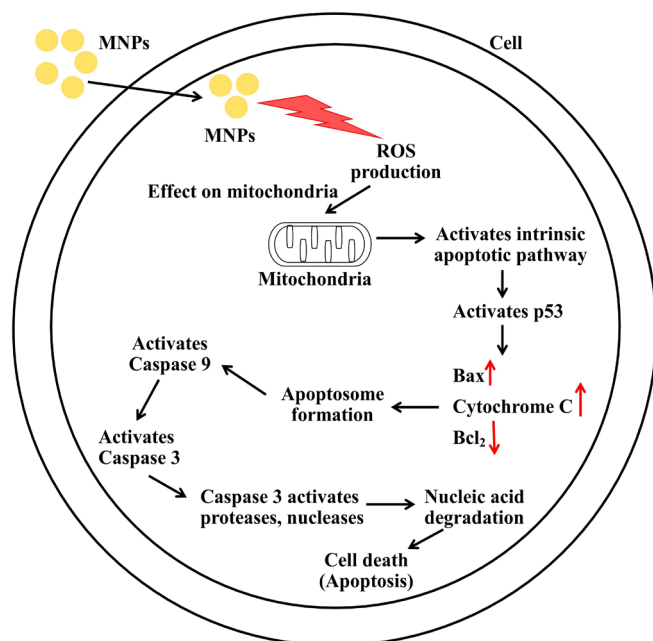


Fig. 4: Metallic nanoparticles mediated apoptosis pathway.

the increased anti-proliferating impact of 5F-PpGNPs over the pure drug would be a significant step toward overcoming chemotherapeutic drug resistance in lung cancer cells and would be of tremendous benefit during lung cancer therapy (Li *et al.*, 2020). Due to their higher metabolic rates and intrinsic higher levels of (mitochondrial) ROS the cancer cells are likely to show an elevated basal level of oxidative stress compared to the normal cell lines. In addition, ROS is generated by the various NPs, resulting in inflated toxic effects compared to non-cancerous counterparts (Han *et al.*, 2014; Maksoudian *et al.*, 2020) (Fig. 4). The previous study reported that the biogenic AgNPs displayed dose-dependent toxicity (50–250  $\mu\text{g}/\text{mL}$ ) against human hepatocellular cancer cell line (HepG2) compared to hepatic fetal human epithelial normal cell-line (WRL-68) (Some *et al.*, 2019). Therefore, MNPs may be used as a noble anti-tumorigenic agent in the field of cancer therapy.

### Anti-parasitic Activity

NPs have recognized new attention as anti-parasitic therapeutic agents. *Entamoeba histolytica* is a hostile protozoan causing amoebic dysentery in developing countries (Showler and Boggild, 2013). *Cryptosporidium parvum* is another pathogenic protozoan causing cryptosporidiosis, a parasitic enteric disease of mammals (Suler *et al.*, 2016). Saad *et al.* (2015) reported that AgNPs exhibited anti-parasitic activity against *Entamoeba histolytica* and *Cryptosporidium parvum*. The LC<sub>50</sub> value of AgNPs was found to be 0.34 and 0.54 mg/l against the above two parasites. Leishmaniasis is an internecine parasitic disease caused by *Leishmania* protozoan and spread by the bite of sand fly (*Phlebotomus* sp.). Skin sores are the symptoms of cutaneous leishmaniasis, and visceral leishmaniasis influences several inner organs such as spleen, liver, etc. (Herwaldt, 1999). The anti-leishmanial potential of bio-compatible AgNPs has also been tested against promastigote of *Leishmania donovani* with an LC<sub>50</sub> value of  $51.88 \pm 3.51 \mu\text{g}/\text{mL}$  compared to its prescribed drug miltefosine (Baranwal *et al.*, 2018). El-Khadragy *et al.* (2018)

suggested that, biogenic AgNPs exhibited outstanding efficacy against *Leishmania major* compared to common antimonial treatment undoubtedly by improving the *in-vivo* antioxidant activity. AgNPs have been revealed to have prominent larvicidal and pupicidal characteristics on the malarial vector *Anopheles stephensi* and dengue vector *Aedes aegypti* at 0.25 percent dosage (Nalini *et al.*, 2017). Toxoplasmosis is another parasitic disease caused by *Toxoplasma gondii*. Alajmi *et al.* (2019) suggested that biosynthesized AgNPs have been used as unique therapeutic attitudes for interference against the progressive liver damage related to toxoplasmosis. Nowadays rapid emergence of drug resistance in the parasite is a major drawback in disease management (Ahmad *et al.*, 2015). Therefore, NPs would be an effective potential against parasites and an alternative larvicide for the control of vector-borne diseases with an eco-friendly approach.

### CONCLUSION

Biosynthesis of NPs is a substitute for traditional chemical and physical methods. Synthesis of different MNPs via the green route is more useful than standard chemical techniques as the green strategy decreases toxic chemicals, heavy pressure, and thermal environments. It also plays a key role in keeping an environmentally friendly strategy in an efficient and manageable period. The rich biodiversity leads to better availability of plants and also the wide variety of alkaloids, flavonoids, terpenoids, phenolic etc. have potent bio-reducing properties in the presence of metallic salts. Especially medicinal plants have great importance for noble biomolecules that exist in the plant extract, which perform as both reducing and stabilizing agents. In this current article, we want to focus on the simple accessibility of raw materials, cost-effectiveness, and eco-friendly nature of the green biosynthesis project. It is also discussed here that green-based synthesis techniques can provide NPs with regulated size and morphology. Additionally, the biosynthesized NPs is indispensable to their potential use in various biomedical applications and in drug delivery. AuNPs and AgNPs are more active against microbes as they have wonderful antimicrobial activity against several bacteria and fungi. Bio-reduced CuNPs, PdNPs, and PtNPs also demonstrated an excellent bactericidal effect against pathogenic microorganisms. *In-vitro* synthesis of MNPs via green route may have a future path towards the efficient use of green synthesized NPs in the shipment of drugs, water treatment, antioxidants, catalysts, anti-inflammatory agents, anti-cancerous drugs, in addition to which the interest is also in the efficient channeling of waste in the atmosphere to safeguard our environment, as this is a subject most discussed and worried around the globe. Hopefully, this article will find a new way for upcoming research and will be a milestone in future Nano-biotechnological research to synthesize MNPs via a green approach.

### Author's Contribution

SS designed the concept. SD arranged the biosynthesis of NPs part. SD and RM prepared the figures and tables. SS and RM arranged the characterization of NPs part. SS and GKB arranged the biocidal of NPs part. SS, RM, and MG wrote the final version of the manuscript with the help of other authors.

## ACKNOWLEDGMENTS

The authors are grateful to Dr. Amit Kumar Mandal, Director, Centre for Nanotechnology Sciences and Assistant Professor, Chemical Biology Laboratory, Department of Sericulture, Raiganj University, West Bengal, India and Prof. Ismail Ocsoy, Department of Analytical Chemistry, Faculty of Pharmacy, Erciyes University, 38039 Kayseri, Turkey for their support and encouragement. RM would like to acknowledge DST India, for Inspire Fellowship (IF190457).

## REFERENCES

- Abbai, R., Mathiyalagan, R., Markus, J., Kim, Y.J., Wang, C., Singh, P., Ahn, S., & Farh M.E. (2016). Green synthesis of multifunctional silver and gold nanoparticles from the oriental herbal adaptogen: Siberian ginseng. *International Journal of Nanomedicine*, 11, 3131-3143.
- Achuthan, S., Chung, B., Ghosh, P., Rangachari, V., & Vaidya, A. (2011). A modified Stokes-Einstein equation for A $\beta$  aggregation. *BMC Bioinformatics*, 12, S13.
- Ahluwalia, V., Elumalai, S., Kumar, V., Kumar, S., & Sangwan, R.S. (2018). Nano silver particle synthesis using *Swertia paniculata* herbal extract and its antimicrobial activity. *Microbial Pathogenesis*, 114, 402-408.
- Ahmad, A., Syed, F., Shah, A., Khan, Z., Tahir, K., Khan, A.U., & Yuan, Q. (2015). Silver and gold nanoparticles from *Sargentodoxa cuneata*: synthesis, characterization and antileishmanial activity. *RSC Advances*, 5, 73793-73806.
- Ahmad, T., Bustam, M.A., Irfan, M., Moniruzzaman, M., Asghar, H., & Bhattacharjee, S. (2019). Mechanistic investigation of phytochemicals involved in green synthesis of gold nanoparticles using aqueous *Elaeis guineensis* leaves extract: Role of phenolic compounds and flavonoids. *Biotechnology and Applied Biochemistry*, 66(4), 698-708.
- Ajitha, B., Reddy, Y.A.K., & Reddy, P.S. (2015). Green synthesis and characterization of silver nanoparticles using *Lantana camara* leaf extract. *Materials Science and Engineering C*, 49, 373-381.
- Akhtar, K., Khan, S.A., Khan, S.B., & Asiri, A.M. (2018). Scanning Electron Microscopy: Principle and Applications in Nanomaterials Characterization. In: Sharma, S. (Ed.) *Handbook of Materials Characterization*, Springer, Cham, pp. 113-145.
- Alajmi, R.A., Al-Megrin, W.A., Metwally, D., Al-Subaie, H., Altamrah, N., Barakat, A.M., Abdel Moneim, A.E., Al-Otaibi, T.T., & El-Khadragy, M. (2019). Anti-Toxoplasma activity of silver nanoparticles green synthesized with *Phoenix dactylifera* and *Ziziphus spina-christi* extracts which inhibits inflammation through liver regulation of cytokines in Balb/c mice. *Bioscience Reports*, 39(5), BSR20190379.
- Amaliyah, S., Pangesti, D.P., Masruri, M., Sabarudin, A., & Sumitro, S.B. (2020). Green synthesis and characterization of copper nanoparticles using *Piper retrofractum* Vahl extract as bioreductor and capping agent. *Heliyon*, 6(8), e04636.
- Anandalakshmi, K., Venugobal, J., & Ramasamy, V. (2016). Characterization of silver nanoparticles by green synthesis method using *Pedalium murex* leaf extract and their antibacterial activity. *Applied Nanoscience*, 6, 399-408.
- Antony, J.J., Sivalingam, P., Siva, D., Kamalakkannan, S., Anbarasu, K., Sukirtha, R., Krishnan, M., & Achiraman, S. (2011). Comparative evaluation of antibacterial activity of silver nanoparticles synthesized using *Rhizophora apiculata* and glucose. *Colloids and Surfaces B: Biointerfaces*, 88, 134-140.
- Aritonang, H.F., Koleangan, H., & Wuntu, A.D. (2019). Synthesis of silver nanoparticles using aqueous extract of medicinal plants' (*Impatiens balsamina* and *Lantana camara*) fresh leaves and analysis of antimicrobial activity. *International Journal of Microbiology*, 2019, 8642303.
- Arya, A., Gupta, K., Chundawat, T.S., & Vaya, D. (2018). Biogenic Synthesis of Copper and Silver Nanoparticles Using Green Alga *Botryococcus braunii* and Its Antimicrobial Activity. *Bioinorganic Chemistry and Applications*, 2018, 1-9.
- Asadabad, M.A., & Eskandari, M.J. (2015). Transmission electron microscopy as best technique for characterization in nanotechnology. *Synthesis and Reactivity in Inorganic, Metal-Organic, and Nano-Metal Chemistry*, 45(3), 323-326.
- Azizi, S., Shahri, M.M., Rahman, H.S., Rahim, R.A., Rasedee, A., & Mohamad, R. (2017). Green synthesis palladium nanoparticles mediated by white tea (*Camellia sinensis*) extract with antioxidant, antibacterial, and antiproliferative activities toward the human leukemia (MOLT-4) cell line. *International Journal of Nanomedicine*, 12, 8841-8853.
- Baldemir, A., Kose, B., Ildiz, N., Ilgun, S., Yusufbeyoglu, S., Yilmaz, V., & Ocsoy, I. (2017). Synthesis and characterization of green tea (*Camellia sinensis* (L.) Kuntze) extract and its major components-based nanoflowers: a new strategy to enhance antimicrobial activity. *RSC Advances*, 7, 44303-44308.
- Banerjee, P., & Nath, D. (2015). A phytochemical approach to synthesize silver nanoparticles for non-toxic biomedical application and study on their antibacterial efficacy. *Nanoscience and Technology*, 2(1), 1-14.
- Baranwal, A., Chiranjivi, A.K., Kumar, A., Dubey, V.K., & Chandra, P. (2018). Design of commercially comparable nanotherapeutic agent against human disease-causing parasite, *Leishmania*. *Scientific Reports*, 8, 8814.
- Beg, M., Maji, A., Mandal, A.K., Das, S., Jha, P.K., & Hossain, M. (2018). Probing the binding of *Spathodea campanulata* leaves extract mediated biogenic potential microbicidal silver nanoparticles to human serum albumin: an insight in the light of spectroscopic approach. *Journal of Luminescence*, 202, 147-156.
- Begum, R., Farooqi, Z.H., Naseem, K., Ali, F., Batool, M., Xiao, J., & Irfan, A. (2018). Applications of UV/Vis Spectroscopy in Characterization and Catalytic Activity of Noble Metal Nanoparticles Fabricated in Responsive Polymer Microgels: A Review. *Critical Reviews in Analytical Chemistry*, 48(6), 503-516.
- Behravan, M., Panahi, A.H., Naghizadeh, A., Ziaee, M., Mahdavi, R., & Mirzapour, A. (2019). Facile green synthesis of silver nanoparticles using *Berberis vulgaris* leaf and root aqueous extract and its antibacterial activity. *International Journal of Biological Macromolecules*, 124, 148-154.
- Benedec, D., Oniga, I., Cuiabus, F., Sevastre, B., Stiuflu, G., Duma, M., Hanganu, D., Iacovita, C., Stiuflu, R., & Lucaciu, C.M. (2018). *Origanum vulgare* mediated green synthesis of biocompatible gold nanoparticles simultaneously possessing plasmonic, antioxidant and antimicrobial properties. *International Journal of Nanomedicine*, 13, 1041-1058.
- Bhagat, M., Anand, R., Datt, R., Gupta, V., & Arya S. (2019). Green Synthesis of Silver Nanoparticles Using Aqueous Extract of *Rosa brunonii* Lindl and Their Morphological, Biological and Photocatalytic Characterizations. *Journal of Inorganic and Organometallic Polymers and Materials*, 29, 1039-1047.
- Bora, T., & Dutta, J. (2014). Applications of nanotechnology in wastewater treatment--a review. *Journal of Nanoscience and Nanotechnology*, 14(1), 613-626.
- Borges, A., Ferreira, C., Saavedra, M.J., & Simões, M. (2013). Antibacterial activity and mode of action of ferulic and gallic acids against pathogenic bacteria. *Microbial Drug Resistance*, 19(4), 256-265.
- Bunaciu, A.A., Udriștioiu, E.G., & Aboul-Enein, H.Y. (2015). X-Ray diffraction: instrumentation and applications. *Critical Reviews in Analytical Chemistry*, 45, 289-299.
- Buszewski, B., Railean-Plugaru, V., Pomastowski, P., Rafiński, K., Szultka-Mlynska, M., Golinska, P., Wypij, M., Laskowski, D., & Dahm, H. (2018). Antimicrobial activity of biosilver nanoparticles produced by a novel *Streptacidiphilus durhamensis* strain. *Journal of Microbiology, Immunology and Infection*, 51, 45-54.
- Chahar, V., Sharma, B., Shukla, G., Srivastava, A., & Bhatnagar, A. (2018). Study of antimicrobial activity of silver nanoparticles synthesized using green and chemical approach. *Colloids and Surfaces A: Physicochemical and Engineering Aspects*, 554, 149-155.
- Chahardoli, A., Karimi, N., & Fattahi, A. (2018). *Nigella arvensis* leaf extract mediated green synthesis of silver nanoparticles: their characteristic properties and biological efficacy. *Advanced Powder Technology*, 29(1), 202-210.
- Chaudhuri, S.K., Chandela, S., & Malodia, L. (2016). Plant mediated green synthesis of silver nanoparticles using *Tecomella undulata* leaf extract and their characterization. *Nano Biomedicine and Engineering*, 8, 1-8.

- Clogston, J. D., & Patri, A. K. (2011). Zeta potential measurement. *Methods in Molecular Biology (Clifton, N.J.)*, 697, 63–70.
- Daphedar, A., & Taranath, T.C. (2018). Characterization and cytotoxic effect of biogenic silver nanoparticles on mitotic chromosomes of *Drimys palyantha* (Blatt. & McCann) Stearn. *Toxicology Reports*, 5, 910–918.
- Das, R.K., Pachapur, V.L., Lonappan, L., Naghdi, M., Pulicharla, R., Maiti, S., Cleon, M., Daila, L.M.A., Sarma, S.J., & Brar, S.K. (2017). Biological synthesis of metallic nanoparticles: plants, animals and microbial aspects. *Nanotechnology for Environmental Engineering*, 2, 18.
- Devaraj, P., Kumari, P., Aarti, C., & Renganathan, A. (2013). Synthesis and characterization of silver nanoparticles using Cannonball leaves and their cytotoxic activity against MCF-7 cell line. *Journal of Nanotechnology*, 2013, 598328.
- Dinesh, M., Roopan, S.M., Selvaraj, C.I., & Arunachalam, P. (2017). *Phyllanthus emblica* seed extract mediated synthesis of PdNPs against antibacterial, hemolytic and cytotoxic studies. *Journal of Photochemistry and Photobiology B*, 167, 64–71.
- Dobrucka, R. (2019). Biofabrication of platinum nanoparticles using *Fumariae herba* extract and their catalytic properties. *Saudi Journal of Biological Sciences*, 26, 31–37.
- Doyle, W.M. (1992). Principles and applications of Fourier transform infrared (FTIR) process analysis. *Proceedings of Control Quality*, 2, 11–41.
- El-Khadragy, M., Alolayan, E.M., Metwally, D.M., El-Din, M., Alobud, S.S., Alsultan, N.I., Alsaif, S.S., Awad, M.A., & Abdel Moneim, A.E. (2018). Clinical efficacy associated with enhanced antioxidant enzyme activities of silver nanoparticles biosynthesized using *Moringa oleifera* leaf extract, against cutaneous Leishmaniasis in a murine model of *Leishmania major*. *International Journal of Environmental Research and Public Health*, 15(5), 1037.
- Elumalai, E.K., Kayalvizhi, K., & Silvan, S. (2014). Coconut water assisted green synthesis of silver nanoparticles. *Journal of Pharmacy & Bioallied Sciences*, 6(4), 241–245.
- Emmanuel, R., Saravanan, M., Ovais, M., Padmavathy, S., Shinwari, Z.K., & Prakash, P. (2017). Antimicrobial efficacy of drug blended biosynthesized colloidal gold nanoparticles from *Justicia glauca* against oral pathogens: a nano-antibiotic approach. *Microbial Pathogenesis*, 113, 295–302.
- Francis, S., Joseph, S., Koshy, E.P., & Mathew, B. (2017). Green synthesis and characterization of gold and silver nanoparticles using *Mussaenda glabrata* leaf extract and their environmental applications to dye degradation. *Environmental Science and Pollution Research International*, 24(21), 17347–17357.
- Geetha, R., Ashokkumar, T., Tamilselvan, S., Govindaraju, K., Sadiq, M., & Singaravelu, G. (2013). Green synthesis of gold nanoparticles and their anticancer activity. *Cancer Nanotechnology*, 4(4–5), 91–98.
- Ghosh, R., Tiwary, B.K., Kumar, A., & Chakraborty, R. (2014). Guava leaf extract inhibits quorum-sensing and *Chromobacterium violaceum* induced lysis of human hepatoma cells: whole transcriptome analysis reveals differential gene expression. *PLoS One*, 9(9), e107703.
- Ghosh, S., Nitnavare, R., Dewle, A., Tomar, G.B., Chippalkatti, R., More, P., Kitture, R., Kale, S., Bellare, J., & Chopade, B.A. (2015). Novel platinum-palladium bimetallic nanoparticles synthesized by *Dioscorea bulbifera*: anticancer and antioxidant activities. *International Journal of Nanomedicine*, 10, 7477–7490.
- Ghranh, H.A., Khan, K.A., & Ibrahim, E.H. (2019). Biological activities of *Euphorbia peplus* leaves ethanolic extract and the extract fabricated gold nanoparticles (AuNPs). *Molecules (Basel, Switzerland)*, 24(7), 1431.
- Gurunathan, S., Kim, E., Han, J.W., Park, J.H., & Kim, J.H. (2015). Green chemistry approach for synthesis of effective anticancer palladium nanoparticles. *Molecules (Basel, Switzerland)*, 20(12), 22476–22498.
- Haggag, E.G., Elshamy, A.M., Rabeih, M.A., Gabr, N.M., Salem, M., Youssif, K.A., Samir, A., Muhsinah, A.B., Alsayari, A., & Abdelmohsen, U.R. (2019). Antiviral potential of green synthesized silver nanoparticles of *Lampranthus coccineus* and *Malephora lutea*. *International Journal of Nanomedicine*, 14, 6217–6229.
- Han, J.W., Gurunathan, S., Jeong, J.K., Choi, Y.J., Kwon, D.N., Park, J.K., & Kim, J.H. (2014). Oxidative stress mediated cytotoxicity of biologically synthesized silver nanoparticles in human lung epithelial adenocarcinoma cell line. *Nanoscale Research Letters*, 9(1), 459.
- Hassanien, R., Husein, D.Z., & Al-Hakkani, M.F. (2018). Biosynthesis of copper nanoparticles using aqueous *Tilia* extract: antimicrobial and anticancer activities. *Heliyon*, 4(12), e01077.
- Hazarika, M., Borah, D., Bora, P., Silva, A.R., & Das, P. (2017). Biogenic synthesis of palladium nanoparticles and their applications as catalyst and antimicrobial agent. *PLoS One*, 12, e0184936.
- Herwaldt, B.L. (1999). Leishmaniasis. *Lancet*, 354, 1191–1199.
- Huo, Y., Singh, P., Kim, Y.J., Soshnikova, V., Kang, J., Markus, J., Ahn, S., Castro-Aceituno, V., Mathiyalagan, R., Chokkalingam, M., Bae, K.S., & Yang, D.C. (2018). Biological synthesis of gold and silver chloride nanoparticles by *Glycyrrhiza uralensis* and in vitro applications. *Artificial Cells, Nanomedicine, and Biotechnology*, 46(2), 303–312.
- Iravani, S., Korbekandi, H., Mirmohammadi, S.V., & Zolfaghari, B. (2014). Synthesis of silver nanoparticles: chemical, physical and biological methods. *International Journal of Research in Pharmaceutical Sciences*, 9(6), 385–406.
- Islam, N.U., Jailil, K., Shahid, M., Rauf, A., Muhammad, N., Khan, A., Shah, M.R., & Khan, M.A. (2019). Green synthesis and biological activities of gold nanoparticles functionalized with *Salix alba*. *Arabian Journal of Chemistry*, 12, 2914–2925.
- Ismail, A.A., Voort van de, F.R., & Sedman, J. (1997). Fourier transform infrared spectroscopy: principles and applications. In: Paré, J.R.J. & Bélanger, J.M.R. (Eds.) *Techniques and Instrumentation in Analytical Chemistry (Volume 18)*, Elsevier B.V., pp.93–139.
- Ismail, E., Saqer, A., Assirey, E., Naqvi, A., & Okasha, R. (2018). Successful green synthesis of gold nanoparticles using a *Corchorus olitorius* extract and their antiproliferative effect in cancer cells. *International Journal of Molecular Sciences*, 19(9), 2612.
- Jamdade, D.A., Rajpali, D., Joshi, K.A., Kitture, R., Kulkarni, A.S., Shinde, V.S., Bellare, J., Babiyi, K.R., & Ghosh, S. (2019). *Gnidia glauca* and *Plumbago zeylanica* mediated synthesis of novel copper nanoparticles as promising antidiabetic agents. *Journal of Advanced Pharmaceutical Science and Technology*, 2019, 9080279.
- Javier, J. (2014). An Introduction to Raman Spectroscopy: Introduction and Basic Principles. <https://analyticalscience.wiley.com/doi/10.1002/sepspec.1882education/full/> (accessed 25<sup>th</sup> December, 2020)
- Jeevanandam, J., Barhoum, A., Chan, Y.S., Dufresne, A., & Danquah, M.K. (2018). Review on nanoparticles and nanostructured materials: history, sources, toxicity and regulations. *Beilstein Journal of Nanotechnology*, 9, 1050–1074.
- Jeyapaul, U., Kala, M.J., Bosco, A.J., Piruthiviraj, P., & Easuraja, M. (2018). An eco-friendly approach for synthesis of platinum nanoparticles using leaf extracts of *Jatropha Gossypifolia* and *Jatropha Glandulifera* and its antibacterial activity. *Oriental Journal of Chemistry*, 34(2), 340223
- Joshi, M., Bhattacharyya, A., & Ali, S.W. (2008). Characterization techniques for nanotechnology applications in textiles. *Indian Journal of Fibre and Textile Research*, 33(3), 304–317.
- Kanchana, A., Devarajan, S., & Ayyappan, S.R. (2010). Green synthesis and characterization of palladium nanoparticles and its conjugates from *Solanum trilobatum* leaf extract. *Nano-Micro Letters*, 2, 169–176.
- Kandi, V., & Kandi, S. (2015). Antimicrobial properties of nanomolecules: potential candidates as antibiotics in the era of multi-drug resistance. *Epidemiology and Health*, 37, e2015020.
- Katifelis, H., Lyberopoulou, A., Mukha, I., Vityuk, N., Grodzyuk, G., Theodoropoulos, G.E., Efstathopoulos, E.P., & Gazouli, M. (2018). Ag/Au bimetallic nanoparticles induce apoptosis in human cancer cell lines via P53, CASPASE-3 and BAX/BCL-2 pathways. *Artificial Cells, Nanomedicine, and Biotechnology*, 29, 1–10.
- Kedi, P.B.E., Meva, F.E., Kotsedi, L., Nguemfo, E.L., Zangueu, C.B., Ntumba, A.A., Mohamed, H.E.A., & Dongmo, A.B. (2018). Eco-friendly synthesis, characterization, *in-vitro* and *in-vivo* anti-inflammatory activity of silver nanoparticle-mediated *Selaginella myosurus* aqueous extract. *International Journal of Nanomedicine*, 13, 8537–8548.
- Khan, I., Saeed, K., & Khan, I. (2017a). Nanoparticles: Properties, applications and toxicities. *Arabian Journal of Chemistry*, 12(7), 908–931.
- Khan, M., Khan, M., Adil, S.F., Tahir, M.N., Tremel, W., Alkhatlan, H.Z., Al-Warhan, A., & Siddiqui, M.R. (2013). Green synthesis of silver nanoparticles mediated by *Pulicaria glutinosa* extract. *International Journal of Nanomedicine*, 8, 1507–1516.

- Khan, N.T., & Mushtaq, M. (2016). Determination of antifungal activity of silver nanoparticles produced from *Aspergillus niger*. *Biology and Medicine*, 9, 363.
- Khan, S.T., Malik, A., Wahab, R., Abd-Elkader, O.H., Ahamed, M., Ahmad, J., Musarrat, J., & Siddiqui, M.A. (2017b). Synthesis and characterization of some abundant nanoparticles, their antimicrobial and enzyme inhibition activity. *Acta Microbiologica et Immunologica Hungarica*, 64, 203–216.
- Kharabi Masooleh, A., AhmadiKah, A., & Saidi, A. (2019). Green synthesis of stable silver nanoparticles by the main reduction component of green tea (*Camellia sinensis* L.). *IET Nanobiotechnology*, 13(2), 183–188.
- Koca, F.D., Yilmaz, D.D., Onmaz, N.E., Yilmaz, E., & Ocsoy, I. (2020). Green synthesis of allicin based hybrid nanoflowers with evaluation of their catalytic and antimicrobial activities. *Biotechnology Letters*, 42(9), 1683–1690.
- Kulkarni, N., & Muddapur, U. (2014). Biosynthesis of metal nanoparticles: a review. *Journal of Nanoscience and Nanotechnology*, 2014, 510246.
- Li, T., Yan, G., Bai, Y., Wu, M., Fang, G., Zhang, M., Xie, Y., Borjigidai, A., & Fu, B. (2020). Papain bio-inspired gold nanoparticles augmented the anticancer potency of 5-FU against lung cancer. *Journal of Experimental Nanoscience*, 15(1), 109–128.
- Lim, J., Yeap, S.P., Che, H.X., & Low, S.C. (2013). Characterization of magnetic nanoparticle by dynamic light scattering. *Nanoscale Research Letters*, 8, 381.
- Liu, Y., Kim, S., Kim, Y.J., Perumalsamy, H., Lee, S., Hwang, E., & Yi, T.H. (2019). Green synthesis of gold nanoparticles using *Euphrasia officinalis* leaf extract to inhibit lipopolysaccharide-induced inflammation through NF- $\kappa$ B and JAK/STAT pathways in RAW 264.7 macrophages. *International Journal of Nanomedicine*, 14, 2945–2959.
- Mackevica, A., Revilla Besora, P., Brinch, A., & Hansen, S.F. (2016). Current uses of nanomaterials in biocidal products and treated articles in the EU. *Environmental Science: Nano*, 3(5), 1195–1205.
- Maji, A., Beg, M., Mandal, A.K., Das, S., Jha, P.K., & Hossain, M. (2017a). Study of the interaction of human serum albumin with *Alstonia scholaris* leaf extract-mediated silver nanoparticles having bactericidal property. *Process Biochemistry*, 60, 59–66.
- Maji, A., Beg, M., Mandal, A.K., Das, S., Jha, P.K., Kumar, A., Sarwar, S., & Chakrabarti, P. (2017b). Spectroscopic interaction study of human serum albumin and human hemoglobin with *Mersilea quadrifolia* leaves extract mediated silver nanoparticles having antibacterial and anticancer activity. *Journal of Molecular Structure*, 1141, 584–592.
- Majumdar, R., Tantayanon, S., & Bag, B.G. (2017). Synthesis of palladium nanoparticles with leaf extract of *Chrysophyllum cainito* (Star apple) and their applications as efficient catalyst for C–C coupling and reduction reactions. *International Nano Letters*, 7, 267–274.
- Maksoudian, C., Saffarzadeh, N., Hesemans, E., Dekoning, N., Buttiens, K., & Soenen, S.J. (2020). Role of inorganic nanoparticle degradation in cancer therapy. *Nanoscale Advances*, 2(9), 3734–3763.
- Maliszewska, I., & Sadowski, Z. (2009). Synthesis and antibacterial activity of silver nanoparticles. *Journal of Physics: Conference Series*, 146, 012024.
- Matei, A., Matei, S., Matei, G., Cogalniceanu, G., & Cornea, C.P. (2020). Biosynthesis of silver nanoparticles mediated by culture filtrate of lactic acid bacteria, characterization and antifungal activity. *The Euro Biotech Journal*, 4(2), 97–103.
- Mokobi, F. (2020). Atomic force microscope (AFM). <https://microbenotes.com/atomic-force-microscope-afm/> (accessed 10<sup>th</sup> February, 2021).
- Mondal, R., Yilmaz, M.D., & Mandal, A.K., (2021). Green synthesis of carbon nanoparticles: characterization and their biocidal properties. Handbook of Greener Synthesis of Nanomaterials and Compounds, 1st ed. Vol. 2. Elsevier, Amsterdam, Netherlands, pp. 277–306.
- Moodley, J.S., Krishna, S.B.N., Pillay, K., Sershen, & Govender, P. (2018). Green synthesis of silver nanoparticles from *Moringa oleifera* leaf extracts and its antimicrobial potential. *Advances in Natural Sciences: Nanoscience and Nanotechnology*, 9, 015011.
- Mourdikoudis, S., Pallares, R.M., & Thanh, N. (2018). Characterization techniques for nanoparticles: comparison and complementarity upon studying nanoparticle properties. *Nanoscale*, 10(27), 12871–12934.
- Murthy, H.C.A., Abebe, B., Prakash, C.H., & Shantaveerayya, K. (2018). A Review on Green Synthesis of Cu and Cu Nanomaterials for Multifunctional Applications. *Materials Science Research India*, 15(3), 279–295.
- Nalini, M., Lena, M., Sumathi, P., & Sundaravadivelan, C. (2017). Effect of phyto-synthesized silver nanoparticles on developmental stages of malaria vector, *Anopheles stephensi* and dengue vector, *Aedes aegypti*. *Egyptian Journal of Basic and Applied Sciences*, 4(3), 212–218.
- Nasiri, S., & Nasiri, S. (2016). Biosynthesis of silver nanoparticles using *Carum carvi* extract and its inhibitory effect on growth of *Candida albicans*. *Avicenna Journal of Medical Biochemistry*, 4(2), 8.
- Nazar, N., Bibi, I., Kamal, S., Iqbal, M., Nouren, S., Jilani, K., Umair, M., & Ata, S. (2018). Cu nanoparticles synthesis using biological molecule of *P. granatum* seeds extract as reducing and capping agent: growth mechanism and photo-catalytic activity. *International Journal of Biological Macromolecules*, 106, 1203–1210.
- Nellore, J., Pauline, C., & Amarnath, K. (2013). *Bacopa monnieri* phytochemicals mediated synthesis of platinum nanoparticles and its neurorescue effect on 1-methyl 4-phenyl 1,2,3,6 tetrahydropyridine-induced experimental parkinsonism in Zebrafish. *International Journal of Neurodegenerative Disorders*, 2013, 972391.
- Nikitina, V.S., Kuz'mina, L., Melent'ev, A.I., & Shendel', G.V. (2007). Antibacterial activity of polyphenolic compounds isolated from plants of Geraniaceae and Rosaceae families. *Prikladnaia Biokhimiia i Mikrobiologiia*, 43(6), 705–712.
- Norton, J.T. (1937). Uses and limitations of X-Ray diffraction methods. *Journal of Applied Physics*, 8, 307–312.
- Ocsoy, I., Tasdemir, D., Mazicioglu, S., Celik, C., Kati, A., & Ulgen, F. (2017a). Biomolecules incorporated metallic nanoparticles synthesis and their biomedical applications. *Materials Letters*, 212, 45–50.
- Ocsoy, I., Yusufbeyoglu, S., Yilmaz, V., McLamore, E.S., Ildiz, N., & Ulgen, A. (2017b). DNA aptamer functionalized gold nanostructures for molecular recognition and photothermal inactivation of methicillin-Resistant *Staphylococcus aureus*. *Colloids and Surfaces B: Biointerfaces*, 159, 16–22.
- Olajire, A.A., Ifediora, N.F., Bello, M.D., & Benson, N.U. (2018). Green synthesis of copper nanoparticles using *Alchornea laxiflora* leaf extract and their catalytic application for oxidative desulphurization of model oil. *Iranian Journal of Science and Technology, Transactions A: Science*, 42, 1935–1946.
- Otunola, G.A., Afolayan, A.J., Ajayi, E.O., & Odeyemi, S.W. (2017). Characterization, antibacterial and antioxidant properties of silver nanoparticles synthesized from aqueous extracts of *Allium sativum*, *Zingiber officinale*, and *Capsicum frutescens*. *Pharmacognosy Magazine*, 13, 201–208.
- Ouda, S.M. (2014). Antifungal activity of silver and copper nanoparticles on two plant pathogens, *Alternaria alternata* and *Botrytis cinerea*. *Research Journal of Microbiology*, 9, 34–42.
- Ovais, M., Khalil, A.T., Islam, N.U., Ahmad, I., Ayaz, M., Saravanan, M., Shinwari Z.K., & Mukherjee, S. (2018). Role of plant phytochemicals and microbial enzymes in biosynthesis of metallic nanoparticles. *Applied Microbiology and Biotechnology*, 102(16), 6799–6814.
- Pantidos, N., & Horsfall, L.E. (2014). Biological synthesis of metallic nanoparticles by bacteria, fungi and plants. *Journal of Nanomedicine & Nanotechnology*, 5, 233.
- Park, H.G. (2003). Nanoparticle-based detection technology for DNA analysis. *Biotechnology and Bioprocess Engineering*, 8, 221–226.
- Prasad, P.R., Kanchi, S., & Naidoo, E.B. (2016). In-vitro evaluation of copper nanoparticles cytotoxicity on prostate cancer cell lines and their antioxidant, sensing and catalytic activity: one-pot green approach. *Journal of Photochemistry and Photobiology B*, 161, 375–382.
- Priyadarshini, J.F., Sivakumari, K., Selvaraj, R., Ashok, K., Jayaprakash, P., & Rajesh, S. (2018). Green synthesis of silver nanoparticles from propolis. *Research Journal of Life Sciences, Bioinformatics, Pharmaceutical and Chemical Sciences*, 4, 23–36.
- Rades, S., Hodoroaba, V.D., Salge, T., Wirth, T., Lobera, M.P., Labrador, R.H., Natte, K., & Behnke, T. (2014). High-resolution imaging with SEM/T-SEM, EDX and SAM as a combined methodical approach for morphological and elemental analyses of single engineered nanoparticles. *RSC Advances*, 4, 49577–49587.

- Rajasekharreddy, P., & Rani, P.U. (2014). Biosynthesis and Characterization of Pd and Pt Nanoparticles Using *Piper betle* L. Plant in a Photoreduction Method. *Journal of Cluster Science*, 25(5), 1377–1388.
- Rajesh, K.M., Ajitha, B., Reddy, Y.A.K., Suneetha, Y., & Reddy, P.S. (2018). Assisted green synthesis of copper nanoparticles using *Syzygium aromaticum* bud extract: physical, optical and antimicrobial properties. *Optik*, 154, 593–600.
- Ranjitha, V., Kalimuthu, K., Chinnadurai, V., Juliet, Y.S., & Saraswathy, M. (2018). Green synthesis and antioxidant analysis of *in-vivo* leaf and *in-vitro* callus of *Tephrosia villosa*. *Pharmacognosy Magazine*, 14(55), 147–153.
- Ravindran, D., Ramanathan, S., Arunachalam, K., Jeyaraj, G.P., Shunmugiah, K.P., & Arumugam, V.R. (2018). Phytosynthesized silver nanoparticles as anti-quorum sensing and antibiofilm agent against the nosocomial pathogen *Serratia marcescens*: an in vitro study. *Journal of Applied Microbiology*, 124(6), 1425–1440.
- Rawani, A., Ghosh, A., & Chandra, G. (2013). Mosquito larvicidal antimicrobial activity of synthesized nanocrystalline silver particles using leaves and green berry extract of *Solanum nigrum* L. (Solanaceae: Solanales). *Acta Tropica*, 128, 613–622.
- Riss, T.L., Moravec, R.A., Niles, A.L., Duellman, S., Benink, H.A., Worzella, T.J., & Minor, L. (2013) [Updated on 1<sup>st</sup> July, 2016]. Cell Viability Assays. In: Markossian, S., Sittampalam, G.S., Grossman, A. et al. (Eds.) *Assay Guidance Manual* [Internet]. Eli Lilly & Company and the National Center for Advancing Translational Sciences. Bethesda (MD), NBK144065.
- Rodríguez-León, E., Rodríguez-Vázquez, B.E., Martínez-Higuera, A., Rodríguez-Beas, C., Larios-Rodríguez, E., Navarro, R.E., López-Esparza, R., & Iñiguez-Palomares, R.A. (2019). Synthesis of gold nanoparticles using *Mimosa tenuiflora* extract, assessments of cytotoxicity, cellular uptake, and catalysis. *Nanoscale Research Letters*, 14, 334.
- Rokade, S.S., Joshi, K.A., Mahajan, K., Patil, S., Tomar, G., Dubal, D.S., Parihar, V.S., Kitture, R., Bellare, J.R., & Ghosh, S. (2018). *Gloriosa superba* Mediated Synthesis of Platinum and Palladium Nanoparticles for Induction of Apoptosis in Breast Cancer. *Bioinorganic Chemistry and Applications*, 2018, 4924186.
- Saad, H.A., Soliman, M.I., Azzam, A.M., & Mostafa, B. (2015). Anti-parasitic activity of silver and copper oxide nanoparticles against *Entamoeba histolytica* and *Cryptosporidium parvum* cysts. *Journal of the Egyptian Society of Parasitology*, 45(3), 593–602.
- Salari, S., Bahabadi, S.E., Samzadeh-Kermani, A., & Yosefzaei, F. (2019). *In-vitro* evaluation of antioxidant and antibacterial potential of green synthesized silver nanoparticles using *Prosopis farcta* fruit extract. *Iranian Journal of Pharmaceutical Research*, 18(1), 430–455.
- Sangoonkar, G.M., & Pawar, K.D. (2018). *Garcinia indica* mediated biogenic synthesis of silver nanoparticles with antibacterial and antioxidant activities. *Colloids and Surfaces B: Biointerfaces*, 164, 210–217.
- Sastry, M., Patil, V., & Sainkar, S.R. (1998). Electrostatically controlled diffusion of carboxylic acid derivatized silver colloidal particles in thermally evaporated fatty amine films. *Journal of Physical Chemistry B*, 102(8), 1404–1410.
- Seah, M.P., & Dench, W.A. (1979). Quantitative electron spectroscopy of surfaces: A standard data base for electron inelastic mean free paths in solids. *Surface and Interface Analysis*, 1(1), 2–11.
- Selvi, B.C.G., Madhavan, J., & Santhanam, A. (2016). Cytotoxic effect of silver nanoparticles synthesized from *Padina tetrastratica* on breast cancer cell line. *Advances in Natural Sciences: Nanoscience and Nanotechnology*, 7, 035015.
- Shah, S., Gaikwad, S., Nagar, S., Kulshrestha, S., Vaidya, V., Nawani, N., & Pawar, S. (2019). Biofilm inhibition and anti-quorum sensing activity of phytosynthesized silver nanoparticles against the nosocomial pathogen *Pseudomonas aeruginosa*. *Biofouling*, 35(1), 34–49.
- Sharma, P., Pant, S., Rai, S., Yadav, R.B., Sharma, S., & Dave, V. (2018). Green synthesis and characterization of silver nanoparticles by *Allium cepa* L. to produce silver nano-coated fabric and their antimicrobial evaluation. *Applied Organometallic Chemistry*, 32, e4146.
- Sharma, V.K., Yngard, R.A., & Lin, Y. (2009). Silver nanoparticles: green synthesis and their antimicrobial activities. *Advances in Colloid and Interface Science*, 145(1–2), 83–96.
- Shende, S., Ingle, A. P., Gade, A., & Rai, M. (2015). Green synthesis of copper nanoparticles by *Citrus medica* Linn. (Idilimbu) juice and its antimicrobial activity. *World Journal of Microbiology & Biotechnology*, 31(6), 865–873.
- Showler, A.J., and Boggild, A.K. (2013). *Entamoeba histolytica*. *Canadian Medical Association Journal*, 185(12), 1064.
- Siddiqi, K.S., Husen, A., & Rao, R.A.K. (2018). A review on biosynthesis of silver nanoparticles and their biocidal properties. *Journal of Nanobiotechnology*, 16(1), 14.
- Singh, A., & Vishwakarma, H.L. (2015). Study of structural, morphological, optical and electroluminescent properties of undoped ZnO nanorods grown by a simple chemical precipitation. *Materials Science-Poland*, 33, 751–759.
- Singh, H., Du, J., & Yi, T.H. (2016). Green and rapid synthesis of silver nanoparticles using *Borago officinalis* leaf extract: anticancer and antibacterial activities. *Artificial Cells, Nanomedicine, and Biotechnology*, 45(7), 1310–1316.
- Singh, H., Du, J., Singh, P., & Yi, T.H. (2017). Ecofriendly synthesis of silver and gold nanoparticles by *Euphrasia officinalis* leaf extract and its biomedical applications. *Artificial Cells, Nanomedicine, and Biotechnology*, 46(6), 1163–1170.
- Singh, J., Dutta, T., Kim, K.H., Rawat, M., Samddar, P., & Kumar, P. (2018). “Green” synthesis of metals and their oxide nanoparticles: applications for environmental remediation. *Journal of Nanobiotechnology*, 16, 84.
- Some, S., Bulut, O., Biswas, K., Kumar, A., Roy, A., Sen, I.K., Mandal, A., Franco, O.L., Agah Ince, I., Neog, K., Das, S., Pradhan, S., Dutta, S., Bhattacharjya, D., Saha, S., Mohapatra, P.K.D., Bhumali, A., Unni, B.G., Kati, A., Mandal, A.K., Yilmaz, M.D., & Ocsy, I. (2019). Effect of feed supplementation with biosynthesized silver nanoparticles using leaf extract of *Morus indica* L. V1 on *Bombyx mori* L. (Lepidoptera: Bombycidae). *Scientific Reports*, 9, 14839.
- Some, S., Sarkar, B., Biswas, K., Jana, T.K., Bhattacharjya, D., Dam, P., Mondal, R., Kumar, A., Deb, A.K., Sadat, A., Saha, S., Kati, A., Ocsy, I., Franco, O.L., Mandal, A., Mandal, S., Mandal, A.K., & Ince, I.A. (2020). Bio-molecule functionalized rapid one-pot green synthesis of silver nanoparticles and their efficacy towards the multidrug resistant (MDR) gut bacteria of silkworms (*Bombyx mori*). *RSC Advance*, 10, 22742–22757.
- Song, Y., Cong, Y., Wang, B., & Zhang, N. (2020). Applications of Fourier transform infrared spectroscopy to pharmaceutical preparations. *Expert Opinion on Drug Delivery*, 17(4), 551–571.
- Sooväli, L., Rööm, E.I., Kütt, A., Kaljurand, I., & Leito, I. (2006). Uncertainty sources in UV-Vis spectrophotometric measurement. *Accreditation and Quality Assurance*, 11, 246–255.
- Stetefeld, J., McKenna, S. A., & Patel, T.R. (2016). Dynamic light scattering: a practical guide and applications in biomedical sciences. *Biophysical Reviews*, 8(4), 409–427.
- Suler, D., Mullins, D., Rudge, T., & Ashurst, J. (2016). *Cryptosporidium parvum* infection following contact with livestock. *North American Journal of Medicine & Science*, 8(7), 323–325.
- Sun, W. (2018). Principles of Atomic Force Microscopy. In: Cai, J. (Ed.) *Atomic Force Microscopy in Molecular and Cell Biology*, Springer, Singapore, pp. 1–28.
- Thakkar, K.N., Mhatre, S.S., & Parikh, R.Y. (2010). Biological synthesis of metallic nanoparticles. *Nanomedicine*, 6(2), 257–262.
- Thanighairassu, R.R., Sivamai, P., Devika, R., & Nambikkairaj, B. (2014). Green synthesis of gold nanoparticles characterization by using plant essential oil *Mentha piperita* and their antifungal activity against human pathogenic fungi. *Journal of Nanomedicine and Nanotechnology*, 5, 229.
- Thirumurugan, A., Aswitha, P., Kiruthika, C., Nagarajan, S., & Christy, A.N. (2016). Green synthesis of platinum nanoparticles using *Azadirachta indica* – An eco-friendly approach. *Materials Letters*, 170, 175–178.
- Tippayawat, P., Phromviyo, N., Boueroy, P., & Chompoosor, A. (2016). Green synthesis of silver nanoparticles in *Aloe vera* plant extract prepared by a hydrothermal method and their synergistic antibacterial activity. *PeerJ*, 4, e2589.
- Tomaszewska, E., Soliwoda, K., Kadziola, K., Tkacz-Szczeszna, B., Celichowski, G., Cichowski, M., Szmaja, W., & Grobelny, J. (2013). Detection limits of DLS and UV-Vis spectroscopy in characterization of polydisperse nanoparticles colloids. *Journal of Nanomaterials*, 2013, 313081.
- Ullah, I., Khalil, A. T., Ali, M., Iqbal, J., Ali, W., Alarif, S., & Shinwari, Z.K. (2020). Green-Synthesized Silver Nanoparticles Induced Apoptotic Cell Death in MCF-7 Breast Cancer Cells by Generating Reactive Oxygen

- Species and Activating Caspase 3 and 9 Enzyme Activities. *Oxidative Medicine and Cellular Longevity*, 2020, 1215395.
- Umer, A., Naveed, S., Ramzan, N., Rafique, M.S., & Imran, M. (2014). A green method for the synthesis of copper nanoparticles using L-ascorbic acid. *Matéria (Rio de Janeiro)*, 19,197–203.
- Velavan, S., & Amargeetha, A. (2018). X-ray diffraction (XRD) and energy dispersive spectroscopy (EDS) analysis of silver nanoparticles synthesized from *Erythrina Indica* flowers. *Nanoscience and Technology*, 5, 1-5.
- Viet, P.V., Nguyen, H.T., Cao, T.M., & Hieu, L.V. (2016). *Fusarium* antifungal activities of copper nanoparticles synthesized by a chemical reduction method. *Journal of Nanomaterials*, 2016, 1957612.
- Wang, C., Mathiyalagan, R., Kim, Y.J., Aceituno, V.C., Singh, P., Ahn, S., Wang, D., & Yang, D.C. (2016). Rapid green synthesis of silver and gold nanoparticles using *Dendropanax morbifera* leaf extract and their anticancer activities. *International Journal of Nanomedicine*, 11, 3691–3701.
- Wang, D., Zhao, L., Ma, H., Zhang, H., & Guo, L.H. (2017). Quantitative Analysis of Reactive Oxygen Species Photogenerated on Metal Oxide Nanoparticles and Their Bacteria Toxicity: The Role of Superoxide Radicals. *Environmental Science & Technology*, 51(17), 10137–10145.
- Wang, E.C., & Wang, A.Z. (2014). Nanoparticles and their application in cell and molecular biology. *International Journal of Integrative Biology*, 6(1), 9–26.
- Wani, I. A., Ahmad, T., & Manzoor, N. (2013). Size and shape dependant antifungal activity of gold nanoparticles: a case study of *Candida*. *Colloids and Surfaces. B, Biointerfaces*, 101, 162–170.
- Zhang, X.F., Liu, Z.G., Shen, W., & Gurunathan, S. (2016). Silver Nanoparticles: Synthesis, Characterization, Properties, Applications, and Therapeutic Approaches. *International Journal of Molecular Sciences*, 17(9), 1534.
- Zheng, J., Nagashima, K., Parmiter, D., de la Cruz, J., & Patri, A. K. (2011). SEM X-ray microanalysis of nanoparticles present in tissue or cultured cell thin sections. *Methods in Molecular Biology (Clifton, N.J.)*, 697, 93–99.